

1 *Type of the Paper (Article)*

2 **PV Microgrid Design for Rural Electrification**

3 **Sivapriya Mothilal Bhagavathy ¹ and Gobind Pillai ^{2,*}**

4 ¹ Energy and Power Group, University of Oxford, Oxford, UK; sivapriya.mothilalbhagavathy@eng.ox.ac.uk

5 ² School of Science and Engineering, Teesside University, Middlesbrough, UK;

6 * Correspondence: g.g.pillai@tees.ac.uk; Tel.: +44-1642-342500

7 Received: date; Accepted: date; Published: date

8 **Abstract:** There are high number of remote villages that still needs electrification in developing
9 countries. Extension of the central electrical power network to these villages is not viable owing to
10 the high costs and power losses involved. Isolated power systems such as rural microgrids based
11 on renewables could be a potential solution. PV technology is particularly suited for countries like
12 India due factors such as the available solar resource, the modularity of the technology and the
13 lowering technology costs. It was identified that unlike larger isolated power systems, rural
14 microgrids have a low energy demand as the loads are mainly residential and street lighting. Hence
15 these microgrids could be of a single-phase configuration. At present the typical procedure followed
16 by planners of rural networks does not consider the importance of PV source siting and optimisation
17 of network structure. An improved design procedure is introduced in this work based on the use of
18 centre of moments for central PV system sizing, simulated annealing for network structure
19 optimisation and load flow based parametric analysis for confirming the PV microgrid structure
20 before detailed software based PV design. Case studies of two remote villages are used to inform
21 and illustrate the design procedure.

22 **Keywords:** Photovoltaic; microgrid; battery bank; rural electrification; voltage profile; generation
23 siting.
24

25 **1. Introduction**

26 As per the World Bank, about 13% of the world population still have no access to electricity.
27 There are more than 30 countries with less than 50% electrification rates [1]. In India, there are still
28 around 31 million village homes which are not yet electrified [2]. Most remote villages in India,
29 which have not yet been electrified have some common characteristics such as [3]:

- 30 • Being located in areas with difficult terrain such as hills, forests, deserts and islands.
31 Being part of a protected forest area could isolate the village and prevent live conductors
32 being drawn through it.
- 33 • Being located far from the nearest existing grid.
- 34 • Very low population (below 500) and low number of households (ranging between 2
35 and 200).
- 36 • Low power demand even in the near future as the loads are mostly lighting.
- 37 • Minimal transport and communication facilities.
- 38 • Low income level and low affordability.
- 39 • Poor literacy levels and technical skills.

40 Due to their remote locations, high costs are involved in grid extension and also high losses will
41 be encountered while transporting power to the village from the central grid. On-site
42 generation/distributed generation (DG) based on renewable sources would be an economic option to
43 enable faster electrification of villages as compared to extension of a central grid [4]. Advantages of
44 distributed generation based rural electrification include energy loss reduction, reliability of supply,

45 reduction of indoor pollution arising from use of conventional fuel (wood or kerosene) for lighting
 46 [5]. Of the renewable energy technologies, photovoltaics (PV) is ideally suited for remote villages due
 47 to the resource availability, its modular nature which makes transportation convenient, the low
 48 maintenance requirement and long life (up to 25 years). More over PV system costs have continually
 49 declined over the last two decades increasing their affordability [6].

50 The supply systems for rural electrification are mostly isolated power systems of capacity
 51 ranging from 1 kW for villages/hamlets to around 100 kW for large islands. Most of these low capacity
 52 systems are single-phase systems with supply duration of around 4-6 hrs per day. Microgrids are
 53 ideally suited for the small power capacity needed by the remote villages in India. A microgrid is a
 54 self-controlled isolated power distribution system, having sources which are based on power
 55 electronics to provide control on flow of real and reactive power, voltage, current etc., loads and
 56 storage devices [7]. To the utility, the microgrid can be thought of as a controlled cell of the power
 57 system. It can be designed to meet their specific needs; such as, enhance local reliability, reduce
 58 feeder losses, support local voltages, provide increased efficiency, voltage sag correction or provide
 59 uninterrupted power supply [8].

60 When the planning of distribution system with DG is considered, the greatest attention should
 61 be paid in the siting and sizing of DG units because their installation in non-optimal locations can
 62 result both in an increase of power losses and reduction of reliability levels [9, 10]. In rural
 63 distribution systems, the resistance in the distribution lines is often larger than, or at least similar to,
 64 the inductive impedance. The distribution line resistance causes a significant proportion of the
 65 voltage drop along the distribution lines as well as of the line losses [11]. The effect becomes
 66 prominent when small amount of power needs to be taken over longer distances as in cases of villages
 67 far from the existing grid poles. The connection of DG can therefore have a significant influence on
 68 the local voltage level [11].

69 Considerable amount of research work has been done in the issue of optimal placement and
 70 sizing of DGs such as PV systems [12-15]. However, these studies were focused on larger capacity
 71 three-phase microgrids, whereas most of the rural electrification systems are single-phase. In the
 72 existing literature, proper tools that will enable the planner to design such small capacity PV
 73 microgrids while satisfying the technical constraints are not available. This study aims to address this
 74 knowledge gap in the planning of PV microgrids, intended for rural electrification. An improved
 75 design procedure is introduced in this work based on the use of centre of moments for central PV
 76 system sizing given the estimate of spatial load distribution, simulated annealing for network
 77 structure optimisation and load flow based parametric analysis for confirming the PV microgrid
 78 structure before detailed software based PV design. Two isolated remote villages in India with
 79 existing PV microgrids namely Ghotiya village, Chattisgarh and Rajmachi village, Maharashtra are
 80 used as case studies. Case studies of Ghotiya village is used to formulate the design procedure and
 81 that of Rajmachi village to illustrate the design procedure. A comparison of industrial standard PV
 82 system design software PVsyst™ and free online tool PVGIS5 for designing the central PV system is
 83 also carried out.

84 The rest of the paper is organised as follows: Section 2 describes the design problem; Section 3
 85 provides details of the case study systems and describes the analysis and design methodologies
 86 followed for formulating the improved PV microgrid design procedure; Results of analysis are
 87 examined in section 4; The improved design procedure is presented in section 5 along with a case
 88 study illustration; Conclusions are drawn in section 5.

89 2. The Design Problem

90 The constraints of microgrid planning are derived from the requirements for a technically
 91 acceptable operation of distribution systems. There are criteria for the dimensioning of the equipment
 92 as well as criteria for a minimum quality of power supply, specified by the voltage quality and the
 93 reliability of power supply. These requirements can be written as follows [16]:

94 Restriction of maximum power flow on every line:

$$95 \quad I_k \leq I_{k,max} \quad k = 1, 2, \dots, N_k \quad (1)$$

96

97 where I_k is the power flowing in the k^{th} line and k is the line number.

98 Restriction of the upper and lower voltage at every node:

99
$$V_{l,\min} \leq V_l \leq V_{l,\max} \quad l = 1, 2, \dots, N_l \quad (2)$$

100

101 where V_l is voltage at the l^{th} node (bus) and l is the node number. A node is the point of consumer
102 connection on the network.103 Restriction of the maximum frequency of interruptions (H_u) and the maximum unavailability
104 (Q_u) for every consumer:

105
$$\begin{aligned} H_{u,m} &\leq H_{u,\max} \\ Q_{u,m} &\leq Q_{u,\max} \quad m = 1, 2, \dots, N_m \end{aligned} \quad (3)$$

106 where m is the month of the year.107 Factors that are to be considered by the planner when designing a rural distribution system are
108 [17]:

- 109
-
- 110
- Voltage drop limits the design: The loads are distributed over large distances, which
111 increase the voltage drop at the extreme consumer point in a radial system.
 - Losses costs are high: Moving relatively small amounts of power over long distances
112 results in losses which are high in proportion to the amount of power delivered.
 - Layout and customers are restricted to the road network.
 - Loads vary from very small single-phase to medium sized three-phase. Water pumps
115 for irrigation purpose may require three-phase supply.
 - Reliability requirements are below average.
- 117

118 The design problem involves answering the questions given the spatial distribution of load and
119 estimate of magnitudes:

- 120
- What should be the network (microgrid) structure?
 - What should be the size of the central PV system?
 - Where the PV system should be located?
 - What should be the specifications of cables, protective equipment?
- 123

124 The inputs needed in the design process are:

- 125
- Spatially distributed 'point' loads and estimate of its magnitudes
 - Location details and/or local resource availability
 - Roads and other obstacles
 - Expected load growth
 - Cost of PV system and power network feeders
 - Installation cost
 - Operating cost
- 131

132 The design objective is to develop an optimal PV microgrid subject to the following constraints:

- 133
- The minimum PV system and battery bank size determined is adequate to ensure
134 continuity of supply to the load
 - Voltage at each bus/node should be within limits
 - Feeder capacity should not be exceeded
 - The energy losses are minimized
 - The PV system design is based on parameters of practical components.
- 138

139

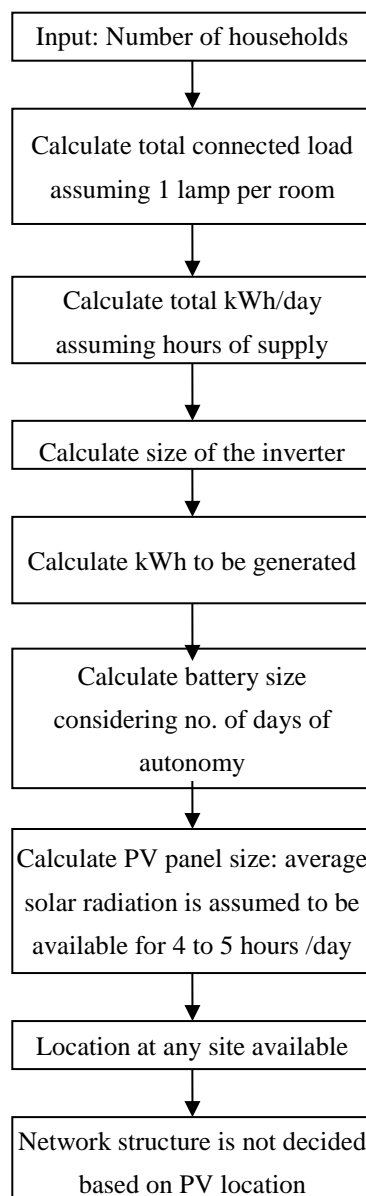
3. Methodology

140 From the literature review, it is observed that no generic set of guidelines are available to help
141 the planner decide the location, size and structure of the PV microgrid for rural electrification. The
142 typical procedure adopted by planners for design of such system is given in Figure 1. The inclusion
143 of power network requirements into the design process is essential to reduce the overall costs, reduce
144 power loss and maximize supply reliability. An improved method for planning is formulated using
145 the case studies of two existing isolated rural power systems in India namely Ghotiya village,

146 Chattisgarh and Rajmachi village, Maharashtra. Optimal location of central PV system as a function
 147 of spatial distribution of load points can be obtained using the centre of moments approach [18].
 148 Network structure is another major issue to be considered in the planning phase of a distribution
 149 system. Given the spatial distribution of system and location of PV system, the optimal network
 150 structure can be obtained using simulated annealing [19]. Parametric analysis using single-phase
 151 power flow can be performed to examine whether the PV system and network structure meets the
 152 technical requirements. In parametric analysis the variation of losses, power generation at slack bus
 153 (bus where the source PV system is connected) and voltage profile with the following parameters is
 154 obtained:

- 155 • Siting of source PV system
- 156 • Size of PV system
- 157 • Slack bus voltage (p. u.)

158 Based on the observations from parametric analysis general rules for sizing and siting of the
 159 central PV system and structure of the network is evolved.



160

161

Figure 1. Typical procedure followed by planners for design of PV based rural electrification.

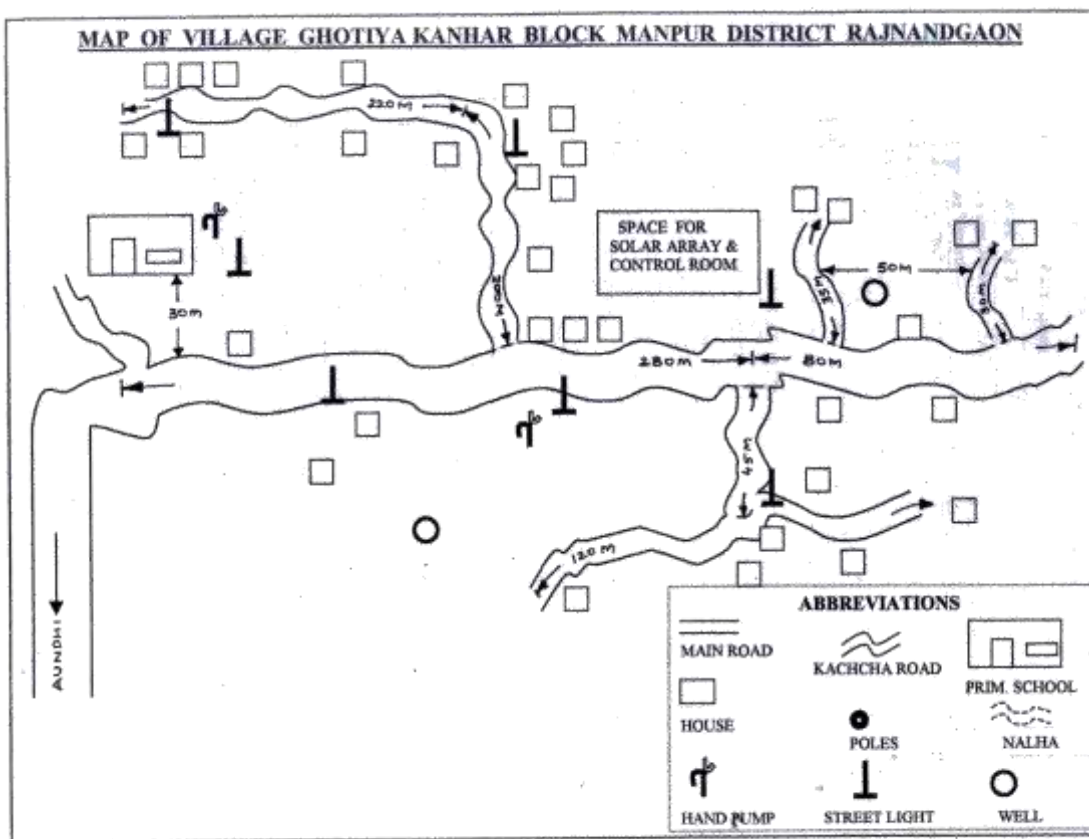
162

163 3.1. Case study systems

164 In the Indian context, there are a large number of villages which are electrified using small
 165 isolated power systems and many more are under the planning stage. To understand the
 166 characteristics of systems for rural electrification systems, two real remote rural isolated networks
 167 were considered as case studies. Their details are as follows:

168 3.1.1. Ghotiya village in Raipur, Chattisgarh

169 The map of Ghotiya village is shown in Figure 2. The geography of the place is covered by dense
 170 forests and mountainous landscape making it an extremely difficult terrain for development
 171 activities. It is difficult to provide grid connectivity from central transmission network of the country
 172 to such villages due to the harsh geographical conditions. Ghotiya was one of the villages electrified
 173 using PV systems by Tata BP Solar Ltd. along with Chattisgarh Renewable Energy Development
 174 Authority (CREDA).



175
 176 **Figure 2.** Map of Ghotiya village (courtesy: CREDA).

177 3.1.2. Rajmachi village near Lonawala, Maharashtra

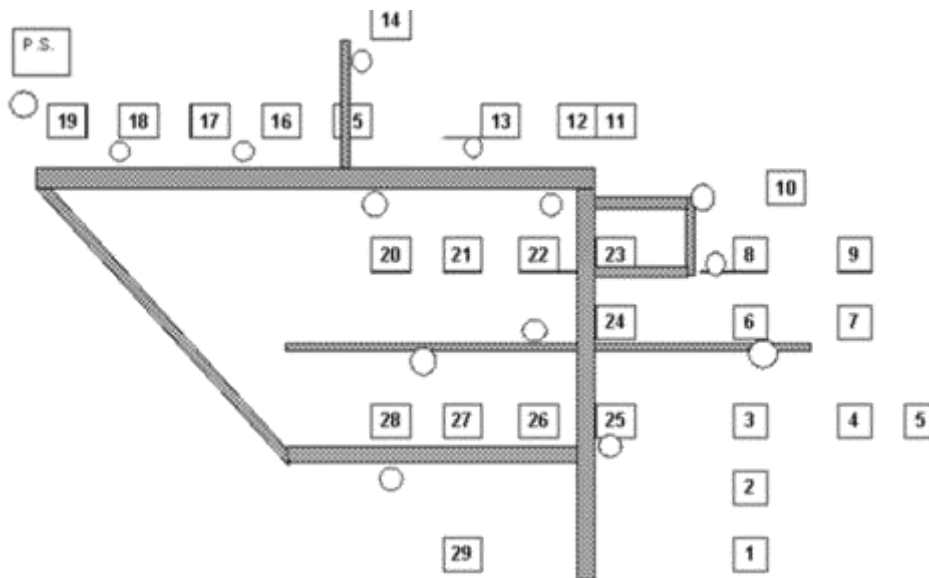
178 Figure 3 shows the village and the extent of isolation of the village. The geography of the location
 179 includes hilly terrain, heavy monsoons, with landslides and continuous rains for 5 to 6 days, making
 180 it more difficult to access the place. Figure 4 gives the map of the village as obtained from MEDA
 181 (Maharashtra Energy Development Agency). Though there are many villages electrified by isolated
 182 power systems, none of them have been documented under running conditions. Hence, the variation
 183 of load (Figure 6) and voltages at different load points over a day for the village microgrid were
 184 documented using the experimental setup shown in Figure 5. The existing PV system which supplies
 185 the village has a rating of 5 kW and a 120 V 800 Ah battery bank. During experimentation, it was
 186 observed that the voltage at the bus furthest from the PV source at near peak load condition is around
 187 210 V. This is 30 V less than the statutory voltage of 240 V. The point is less than 500 m from source.

188 The impedance of the line was calculated as around 8.6 ohms/km ($7.4 + 4.3i$) which is quite high as
189 compared to the central electricity utility recommended distribution line resistance of 1.88 ohms/km.



190
191
192

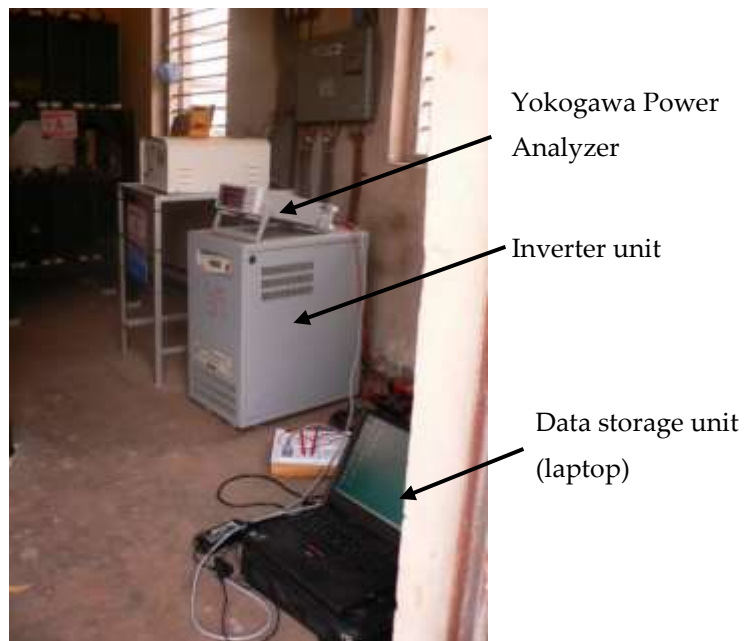
Figure 3. An aerial view of Rajmachi village, Maharashtra.



193
194

Figure 4. Map of Rajmachi village showing the customer load points (courtesy: MEDA).

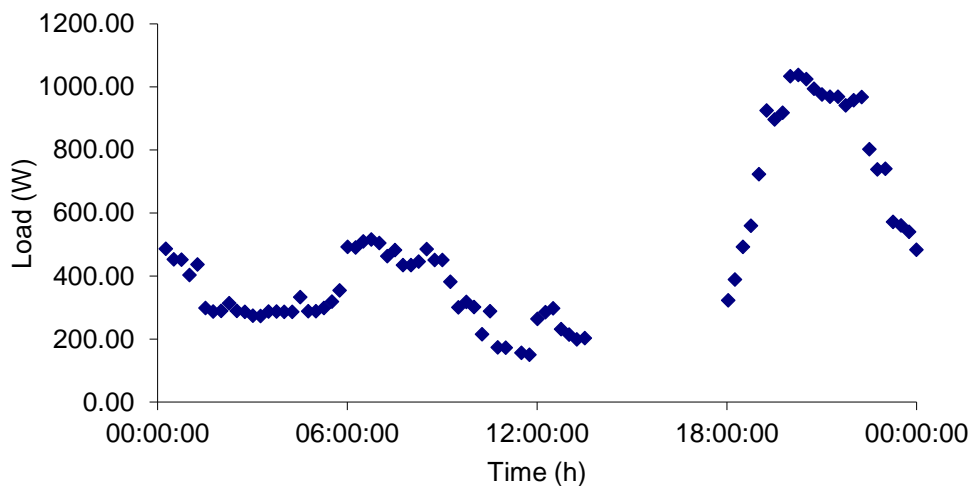
195



196

Figure 5. Experimental setup to analyse the load and voltage profiles.

197



198

Figure 6. Load profile of the existing distribution system of Rajmachi village.

199

3.2. PV system location siting using centre of moments

200

In a power system, the power loss in a line is proportional to the line current and the distance between the two points. The system can be represented in a 2-dimensional space as point loads with a weight equal to the load at each point. Assuming a constant power factor, point loads can be represented by their active power consumption in watts. For total loss of the system to minimum, sum of weighted distances of load from source should be minimum. The optimal location of the source (central PV system) can be obtained by finding out the centre of moments of the points assuming the weights associated with each point as its mass [18].

207

3.3. Network topology design

208

The structure of the power network (topology) should be such that feeders should be able to cover the whole area where service is to be provided and include all the houses in that area. In case of rural feeder design, the two major goals are: cost should be minimized and electrical performance

209

210

211 must be satisfactory. “Backward-Trace” layout procedure generally produces the best results for
 212 finding an optimal network structure. The procedure to find the configuration with least cost is [17]:

- 213 1. Identify all the geographic constraints – areas that cannot be crossed, areas where construction
 214 is not possible etc.
- 215 2. Identify all special opportunities – diagonal routes which contribute to lower cost.
- 216 3. Identify a set of load points on the periphery of the area to be served by the feeder, as well as a
 217 load point that is the “worst case” in terms of each constraint
- 218 4. One by one for each load points identified in step 3, work backward from it toward the
 219 substation (power source) trying to find out the shortest route(s). As feeders generally follow
 220 roads it is better to consider $D = |X| + |Y|$ than $D = \sqrt{|X|^2 + |Y|^2}$ (X and Y are the feeder length
 221 along the 2 coordinates of the site map).
- 222 5. As a shortest path from each point is traced, commonalities among the paths can be used as
 223 major trunk or branch routes.

224 Simulated annealing is a mathematical optimisation technique that mimics the process that
 225 misplaced atoms in a metal undergo, when the metal is slowly cooled after heating. Simulated
 226 annealing is able to find a near optimal solution even with a large number of variables and noisy data
 227 [20]. The quality of the solution provided by this algorithm is dependent on the amount of time it is
 228 given to solve the optimization problem. In this study, simulated annealing was carried out using an
 229 early version of ViPORA (Village Power Optimization Tool box, from NREL) as the authors were
 230 conversant with the software. However, users do not have to restrict to this software as there are a
 231 number of other software such as MATLAB, Global Optimization Software etc. that allow users to
 232 solve optimization problems using simulated annealing. NREL has now replaced ViPORA with
 233 REOPT™ (Renewable Energy Integration and Optimization) software.

234 To determine the cost and the ideal layout of the distribution grid, ViPORA requires a spatial or
 235 description of the village which must include the location and type of each load point (such as houses,
 236 schools, stores etc.) and at least one potential centralized power source location. The spatial
 237 description may also include linear features (such as roads, rivers, and shorelines) and terrain
 238 information. Other inputs needed include:

- 239 • the type of source and cost of generating electricity
- 240 • the costs of running wire across different types of terrain
- 241 • the maximum low voltage line length. This input restricts the length of low voltage wire
 242 runs. It refers to the length of wire between a load point and the transformer to which
 243 it is connected. This restriction is meant to limit voltage drops and line losses.

244 At the end of the simulated annealing process, ViPORA displays a map of the optimal network
 245 structure. The distribution network follows the road wherever possible in order to avoid more
 246 expensive terrain. A breakdown of the costs and revenues associated with the optimal solution can
 247 also be obtained.

248 3.4. Parametric analysis based on load flow

249 To obtain the steady state parameters of a power network, load flow analysis needs to be done.
 250 Load flow analysis of the system gives an efficient way to the following by phase and total three-
 251 phase:

- 252 • Voltage magnitudes and angles at all nodes of the feeder
- 253 • Line flow in each line section specified in kW and kVAr, amps and degree, or amps and
 254 power factor
- 255 • Power loss in each line section
- 256 • Total feeder input kW and kVAr
- 257 • Total feeder power loss
- 258 • Load kW and kVAr based upon the specified model for the load.

259 Normally load flow analysis is conducted for three phase systems, with the assumption that the
 260 phases are balanced and can be represented by a single phase. Owing to this feature, the single phase
 261 network considered in this study can also be analysed by standard balanced load flow algorithms. In
 262 this study, the Gauss-Seidel method of balanced load flow analysis [21] was conducted using the
 263 standard MATLAB code available in free software MATPOWER [22].

264 In distribution networks, which are more resistive, the active power injection will affect the
 265 voltage profile throughout the grid and as the active power injected varies the losses in the system
 266 also vary. For the same network topology the optimal placement is different for different load
 267 profiles. In such a case the PV source should be placed such that voltage drops at any point at the
 268 worst case is within the limits. Hence, the parametric analysis of this study focuses on the node
 269 voltages and total feeder power loss with regards to the location of the PV source. As the PV
 270 microgrid is single-phase in nature, single-phase load flow analysis is performed.

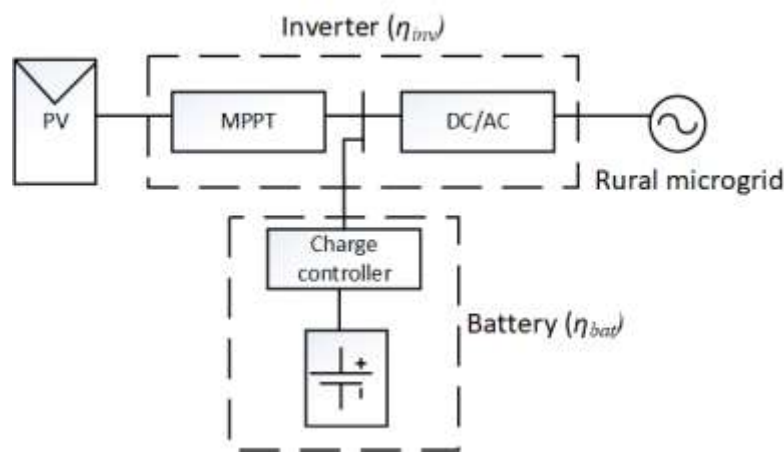
271 3.5. PV system sizing

272 3.5.1. Pre-sizing

273 Pre-sizing of the central PV system has to be based on the load curve of the remote village for a
 274 typical day. A block diagram of the PV system with its main components are shown in Figure 7. The
 275 area under the curve gives the total kWh required per day (E_d). The total energy to be generated per
 276 day by the PV array ($kWh/day_{to\ be\ generated}$) is determined using the inverter efficiency (η_{inv}) as:

277
 278
$$kWh/day_{to\ be\ generated} = \frac{E_d}{\eta_{inv} \times \eta_{bat}} \tag{4}$$

279
 280 The value of η_{inv} is specific to the PV technology used (monocrystalline, polycrystalline,
 281 amorphous etc.) and the inverter topology (H5, HERIC etc. [23]). η_{bat} is the battery round trip
 282 efficiency (the fraction of energy put into the storage that can be retrieved). An η_{bat} of 80% can be
 283 assumed for lead acid batteries commercially available at present. With the current commercially
 284 available inverters, efficiency does not fall below 80% during PV generation hours.



299 **Figure 7.** Block diagram of the central PV system with its main components.

300
 301 The average daily energy from incident global solar insolation (I_t , unit kW/m²) at the location can
 302 be identified from meteorological data or onsite recording using pyranometers. The average daily
 303 photovoltaic energy conversion efficiency (η) will depend mainly on the PV array orientation (tilt and
 304 azimuth) and the PV technology. An η of 10% can be assumed for crystalline silicon with the current
 305 commercially available PV modules. The area of PV array is then calculated as:

306
$$Area = \frac{(kWh/day_{to\ be\ generated})}{I_t \times t \times \eta} \tag{5}$$

307 where t is the average daily sunshine hours over the year.

308 As PV is the only source of power it is essential to include a battery bank to ensure continuity of
 309 supply. The battery size depends on the number of days of autonomy required and the permissible
 310 battery Depth of Discharge (DOD). For remote villages in India the battery technology to be
 311 considered is lead acid due to the low cost and easy availability. Lead acid batteries degrade quickly
 312 if they are completely discharged frequently. So a DOD limit of 40% is imposed. The battery size is
 313 calculated as:

$$314 \quad B = \frac{\left(\frac{kWh}{\text{day to be generated}} \right) \times \text{No. of days of autonomy}}{\text{Battery DOD}} \quad (6)$$

315 Typical lead acid battery has terminal voltage of 2 V/cell and 900 Ah @ C10 (i.e. it can supply at the
 316 rate of 90 A/h for 10 hours before getting fully discharged).

317 3.5.2. Detailed design

318 The PV system pre-sizing does not take into account the variability of the solar resource over the
 319 year. This can lead to over/underestimating the PV system size. While overestimation is financially
 320 unfavourable, underestimating can cause continuity of supply issues in months with lower solar
 321 insolation. Therefore, the availability of weather data (mainly irradiation and temperature data) for
 322 a typical meteorological year and its use in system sizing is essential. JRC (EU Joint Research Centre,
 323 Ispra) has recently released a solar dataset, SARAH which provides data for Europe, Africa, a large
 324 proportion of Asia and parts of South America [24]. The dataset is within PVGIS Climate –SAF
 325 (Photovoltaic Geographical Information System Climate Monitoring Satellite Application Facility),
 326 has a high temporal and spatial resolution and is available free of charge. JRC also provides PVGIS 5,
 327 which is a set of web-based tools for the assessment of PV systems and solar resource [25].

328 PVSyst™ is one of the standard software that is commonly used for design and optimisation of
 329 the PV system operation. It has been validated for different climates and PV module and inverter
 330 technologies and has an inbuilt library of currently available PV modules and inverters [26]. PVSyst™
 331 has the facility to input meteorological data manually from different databases. For the remote village
 332 location considered, the annual energy generation for the pre-sized PV system design can be
 333 simulated using PVSyst™ based on data imported from PVGIS SARAH database. As PVSyst™
 334 simulation considers commercially available modules and inverter parameters it can be used to
 335 modify and finalize the PV system design. For remote rural system design in India, the cost of the
 336 software could be excessive for it to be used in the PV microgrid planning stage. In such case, the
 337 web-based tools of PVGIS could be a viable alternate. Georgitsioti [27] identified that difference in
 338 PV system annual energy outputs simulated by PVGIS only differs by a few percentage from
 339 PVSyst™ outputs.

340 4. Results and Discussion

341 4.1. Location of PV system and determination of network structure

342 4.1.1. Location of central PV system in terms of spatial distribution of load

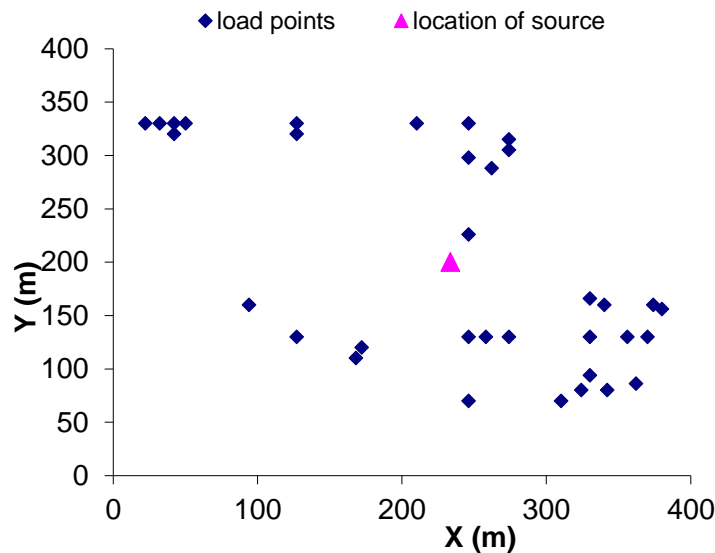
343 One of the specific objectives of the study is to determine the location of the source in terms of
 344 the spatial distribution of loads and also the network structure. Figure 8 shows the map of Ghotiya
 345 village with dark blue dots representing the location of houses. The load at each house has been
 346 considered as two CFL lamps each of 11 W rating and a table fan of 20 W rating (total 42 W).

347 Algebraic sum of all moments around y-axis and x-axis are calculated and divided by the total
 348 load respectively to get the X and Y co-ordinates of the source as discussed in section 3.2 using the
 349 following equation:

$$350 \quad x_{source} = \frac{\sum_{i=1}^N x_i \times P_i}{\sum_{i=1}^N P_i}, \quad y_{source} = \frac{\sum_{i=1}^N y_i \times P_i}{\sum_{i=1}^N P_i} \quad (7)$$

351 where, x_i is the x-co-ordinate of the i^{th} load (P_i), y_i is the y- co-ordinate of the i^{th} load and N is the
 352 total number of loads.

353 The magenta triangle shown on Figure 8 represents the ideal central PV system location arrived
 354 at using the center of moments approach. The central PV system in Ghotiya village should be located
 355 as close to this as possible depending on the availability of land and source of energy so that total
 356 losses are minimized.



357 **Figure 8.** Spatial distribution of load points on the map of village and location of source. The X-axis
 358 shows the distance of load or source points from the estimated origin of the map in the west to east
 359 direction. The Y-axis shows the distance of load or source points from the estimated origin of the map
 360 in the south to north direction.

361 4.1.2. Determination of network topology using simulated annealing

362 The map of Ghotiya village, the location, the load points and that of central PV system based on
 363 the center of moments approach (Figure 8), information about load sizes, equipment costs, terrain
 364 information, low voltage conductor data (sizes, voltage limits and costs) were used as the inputs to
 365 ViPOR software. The costs were taken from a sample system in ViPOR itself. Figure 9 shows the
 366 network structure for the isolated remote rural microgrid system with a central PV source generated
 367 by ViPOR. The data shown as green circles indicate that these are houses, triangle indicates the
 368 location of source and the blue lines represents the network feeder lines.

369 4.1.2. Parametric analysis using load flow

370 To estimate the steady state parameters of the network, a single phase Gauss-Seidel load flow
 371 analysis is used. Table 1 gives the branch data for the network developed for Ghotiya village. Bus no.
 372 12 corresponds to the source location near to the point obtained by the centre of moments approach.
 373 In order to analyse the impact of the PV source location on voltage profile and losses, the load flow
 374 algorithm was run multiple times. The node on which the central PV system is connected (slack bus)
 375 was changed in each run of the load flow program until all nodes were covered. Furthermore, the
 376 location variation analysis was conducted with different load levels in order to identify the impact of
 377 loading levels on the PV source location.

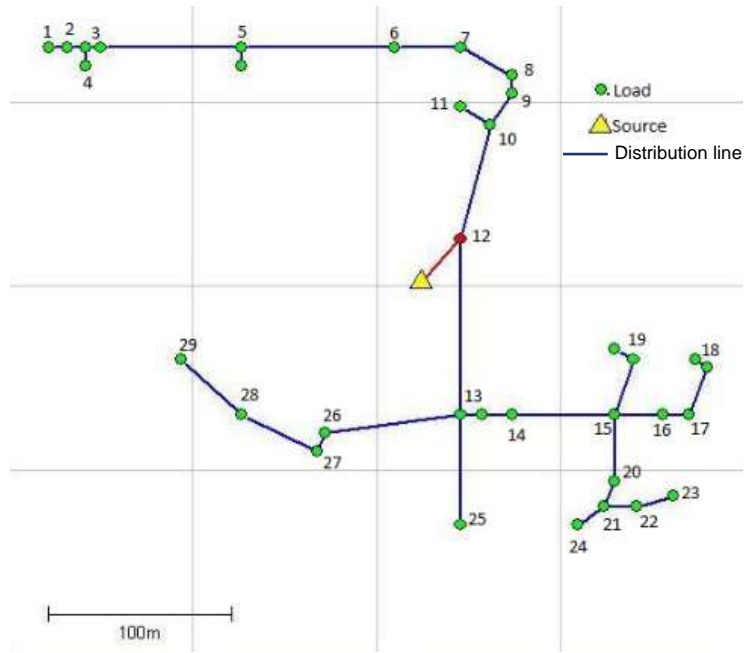


Figure 9. Network structure obtained using simulated annealing.

378
379
380

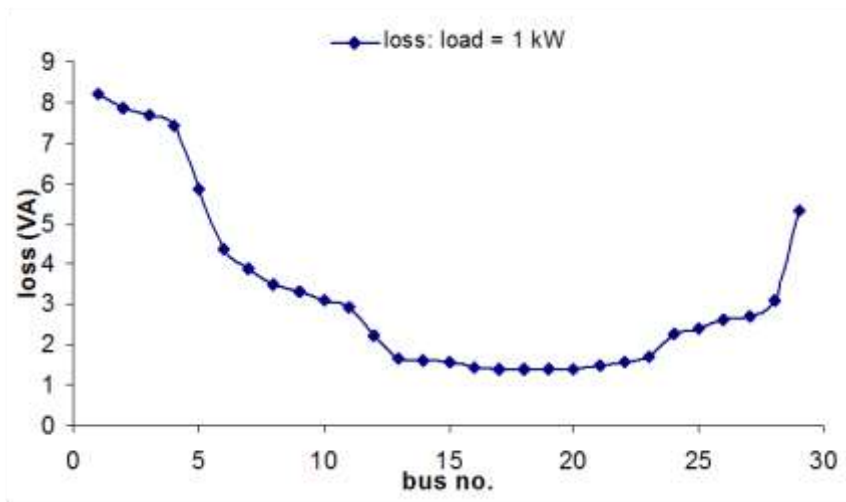
Table 1. Branch data for the Ghotiya village network.

| From | To | Distance (m) | R (in p.u.) | X (in p.u.) |
|------|----|--------------|-------------|-------------|
| 1 | 2 | 11 | 0.013 | 0.011 |
| 2 | 3 | 11 | 0.013 | 0.011 |
| 3 | 4 | 12 | 0.015 | 0.012 |
| 3 | 5 | 78 | 0.095 | 0.076 |
| 5 | 6 | 78 | 0.095 | 0.076 |
| 6 | 7 | 59 | 0.072 | 0.057 |
| 7 | 8 | 42 | 0.051 | 0.041 |
| 8 | 9 | 12 | 0.015 | 0.012 |
| 9 | 10 | 31 | 0.038 | 0.030 |
| 10 | 11 | 31 | 0.038 | 0.030 |
| 10 | 12 | 77 | 0.094 | 0.075 |
| 12 | 13 | 94 | 0.115 | 0.091 |
| 13 | 14 | 17 | 0.021 | 0.016 |
| 14 | 15 | 56 | 0.068 | 0.054 |
| 15 | 16 | 26 | 0.032 | 0.025 |
| 16 | 17 | 13 | 0.016 | 0.013 |
| 17 | 18 | 38 | 0.046 | 0.037 |
| 15 | 19 | 39 | 0.048 | 0.038 |
| 15 | 20 | 35 | 0.043 | 0.034 |
| 20 | 21 | 20 | 0.024 | 0.019 |
| 21 | 22 | 19 | 0.023 | 0.018 |
| 22 | 23 | 19 | 0.023 | 0.018 |
| 21 | 24 | 27 | 0.033 | 0.026 |

| | | | | |
|----|----|----|-------|-------|
| 13 | 25 | 59 | 0.072 | 0.057 |
| 13 | 26 | 83 | 0.101 | 0.080 |
| 26 | 27 | 14 | 0.017 | 0.014 |
| 27 | 28 | 56 | 0.068 | 0.054 |
| 28 | 29 | 63 | 0.077 | 0.061 |

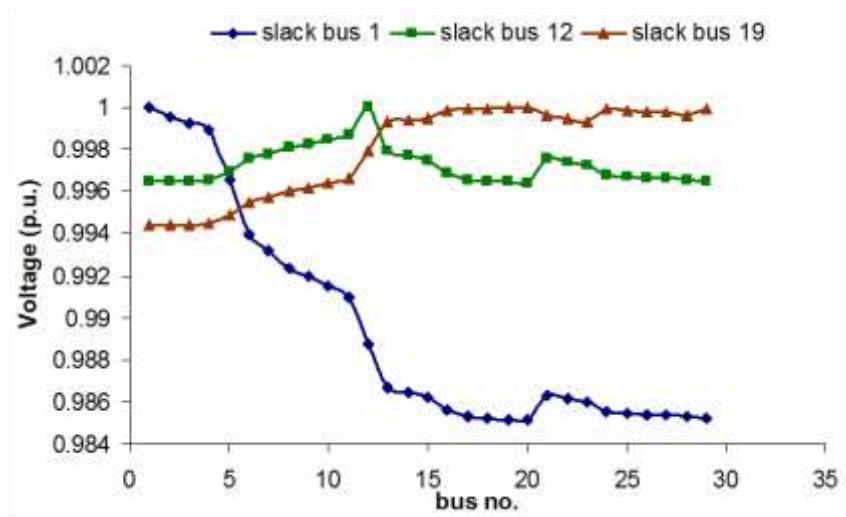
381
382
383
384
385
386

As the system is rural, a fixed power factor of 0.6 pf lagging was considered. Three values of total connected load of 1 kW, 5 kW and 10 kW were considered. Figures 10, 12 and 14 shows the variation of apparent power losses with location of PV source for the respective loading levels. Figures 11, 13, 15 shows the variation of voltage profile with location of PV source for the respective loading levels.



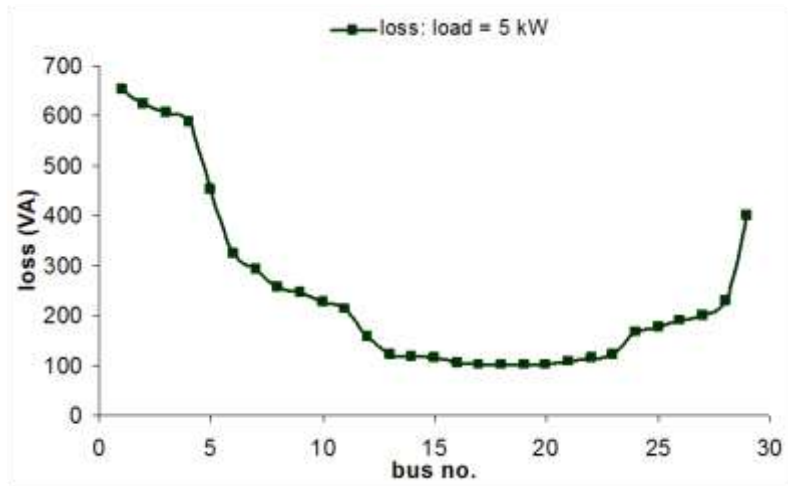
387
388

Figure 10. Variation of losses with location of PV system for a load of 1kW.



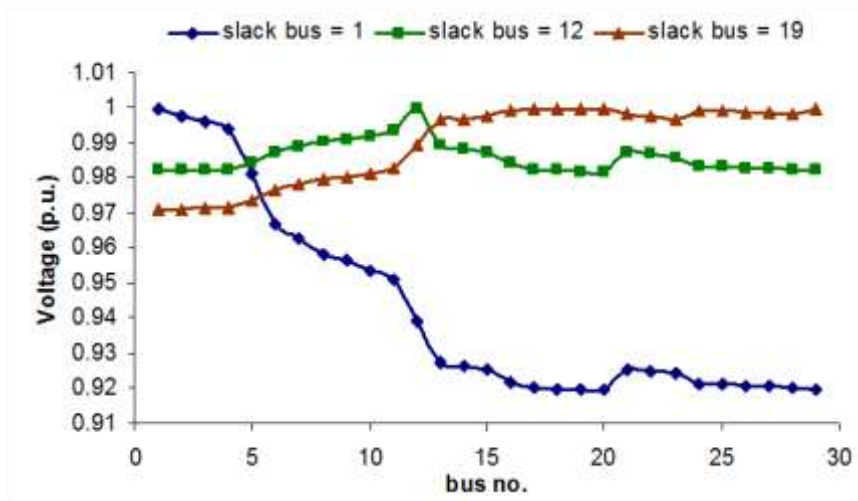
389
390
391

Figure 11. Variation of voltage profile with location of PV system for a load of 1kW.



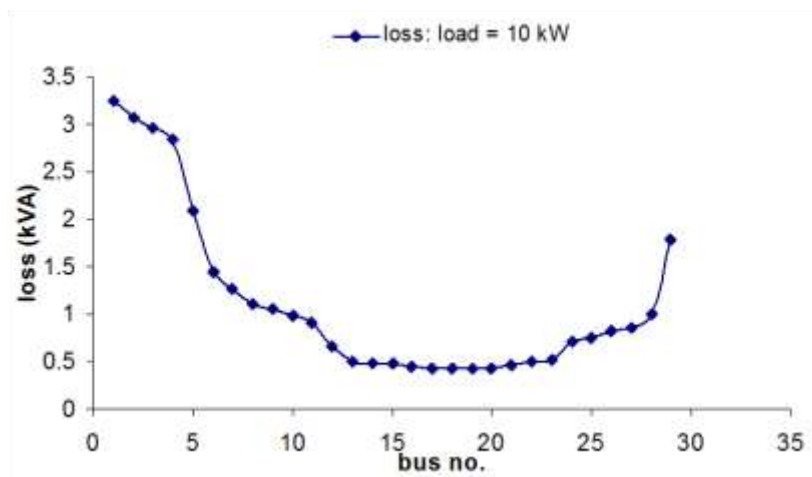
392
393

Figure 12. Variation of losses with location of PV system for a load of 5kW.



394
395

Figure 13. Variation of voltage profile with location of PV system for a load of 5kW.



396
397

Figure 14. Variation of losses with location of PV system for a load of 10kW.

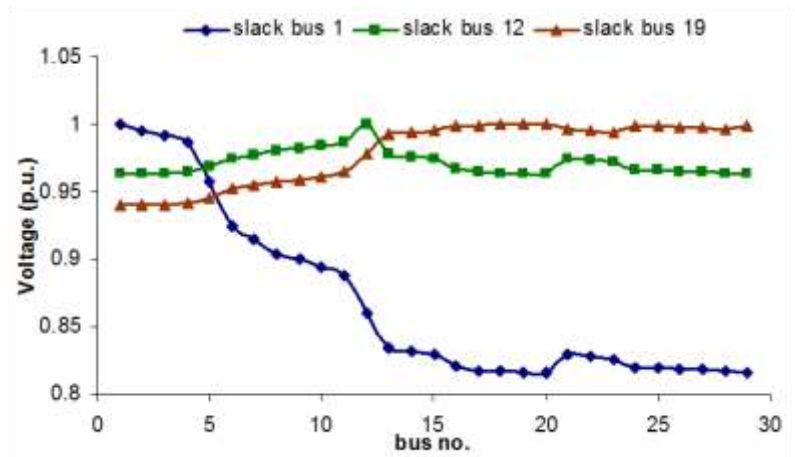


Figure 15. Variation of losses with location of PV system for a load of 10kW.

398
399

400 The losses amount to only 1% of total load when the total connected load considered is 1 kW.
401 However, the percentage reduction in losses is high (around 80%) when placement of the PV source
402 is varied from bus no. 1 to bus no. 19. In this case economics will play a major role as the absolute
403 value of the losses is very small.

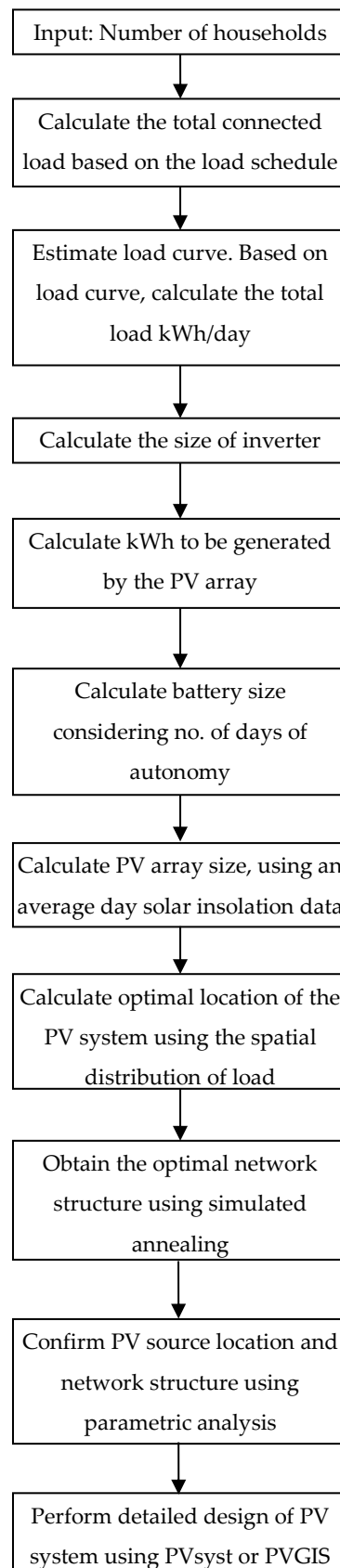
404 As the load is increased from 1 kW to 5 kW, it can be observed that the voltage at the extreme
405 buses tend to drop below 0.95 p.u. which is not acceptable. Here again the percentage reduction of
406 losses is around 80% and the total loss amounts to around 8% of total load when placed in bus no. 1.

407 When the load is increased from 5 kW to 10 kW it can be observed that the total losses accounts
408 to around 20% of the total connected load. Hence in this system both losses and voltage profile need
409 to be considered for optimization. A total connected load of 10 kW is at the higher end of loading
410 level. Normally, when the load increases, the spatial distribution of loads and the area covered by the
411 system increase. When the feeder lengths increase, voltage drop will become a more stringent
412 constraint and losses may account for more than 20% of the total load.

413 From Figure 14 it can be observed that even when the load is increased to 10 kW the voltage
414 drop remains within limits when the PV source is connected to bus no. 12 as compared to bus no. 1.
415 This confirms that the PV source location and network structure determined in section 4.1.1 and 4.1.2
416 is optimal.

417 **5. PV microgrid design method for rural electrification**

418 Based on the analysis presented in section 4.1.1-4.1.3 and findings from literature, an improved
419 method for design of isolated PV microgrids for rural electrification is proposed as in Figure 16.



420

421

Figure 16. Proposed method for planning of isolated PV microgrids for rural electrification.

422 5.1. Illustration of proposed method

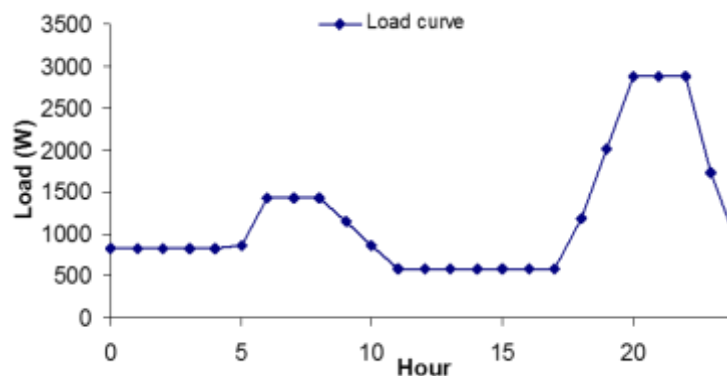
423 For illustration purpose, it is assumed that the village of Rajmachi, Maharashtra is yet to be
 424 electrified. The map as obtained from MEDA (Figure 4) is used. The details of the total connected
 425 load estimation are given in Table 2. The total connected load is around 3 kW. The load curve
 426 obtained from the case study (Figure 6) is normalized and then multiplied with 3 to get the load curve
 427 for the estimated connected load as shown in Figure 17.

428

429

Table 2. Load data of Rajmachi village.

| Load | No. of units | Wattage | Coverage (fraction) | Connected load (W) | No. of households | Total |
|-------------------|--------------|---------|---------------------|--------------------|-------------------|-------|
| Domestic lighting | 3 | 11 | 1 | 33 | 29 | 957 |
| Street lights | 1 | 11 | 0.5 | 5.5 | 29 | 159.5 |
| Fans | 1 | 40 | 0.5 | 20 | 29 | 580 |
| Refrigeration | 1 | 100 | ---- | 100 | 29 | 100 |
| Television | 1 | 80 | 0.4 | 32 | 29 | 928 |
| Radio | 1 | 5 | 0.4 | 1.75 | 29 | 58 |
| Other loads | 1 | 100 | 0.1 | 10 | 29 | 290 |



430

431

Figure 17. Load curve for the system considered.

432 The area under the curve gives the total kWh required per day which is 28.5 kWh for the
 433 considered case. Inverter and battery round trip efficiencies are assumed to be 80%; this gives the
 434 total energy to be generated per day as 44.5 kWh. The total global horizontal irradiation energy
 435 available over PV generation hours (E_d) at the location is 5.037 kWh/m²/day (source PVGIS CMSAF).
 436 Considering monocrystalline PV technology, the average daily system efficiency (η) is assumed as
 437 10%. The PV array is calculated using (4) as approx. 88 m². A generic 75 Wp monocrystalline PV
 438 module of length 1208 mm and width 538 mm is considered. For an area of 10 m², a series parallel
 439 arrangement of the 75 Wp module is equivalent to 1 kWp. Hence the rating of the central PV system
 440 for Rajmachi is estimated as 8.9 kWp. Battery size calculated using (5) lead to an energy rating of 223
 441 kWh. The autonomy considered was 2 days. The battery bank voltage is assumed to be 48 V. This
 442 gives the battery bank specification as 24 cells in series and 6 such strings in parallel.

443

444

445

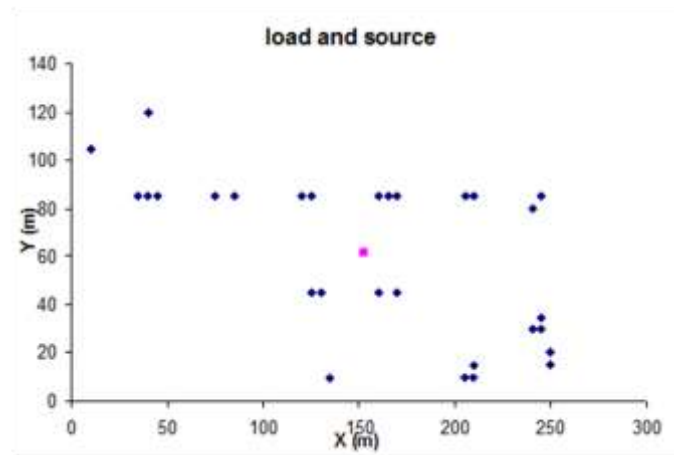
446

447

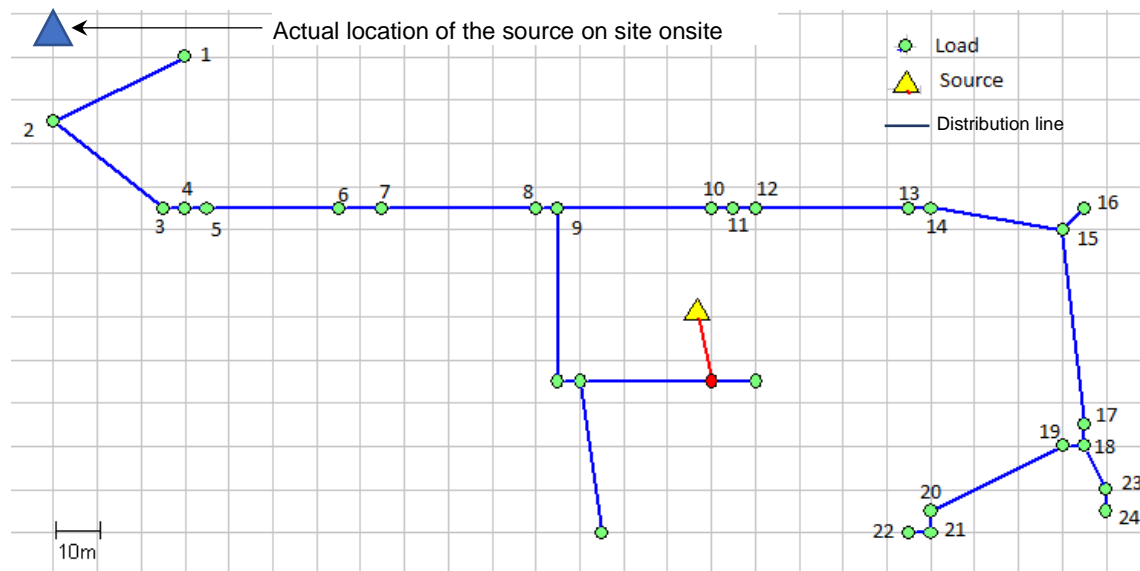
448

The map of the village and the load magnitudes is used to calculate the location of the source which reduces the total losses (using the centre of moments approach). The load points and the PV system location determined are shown in Figure 18. These are given as input to ViPOR for determining the network structure. In the ViPOR simulation, the connected load is clubbed at some points where the distance between the houses is less than 5 m. The optimum network structure obtained using simulated annealing is shown in Figure 19. The actual source location at the village

449 site is also shown. Evidently, the actual source location is not optimum as the total loss in the system
 450 is not minimized.

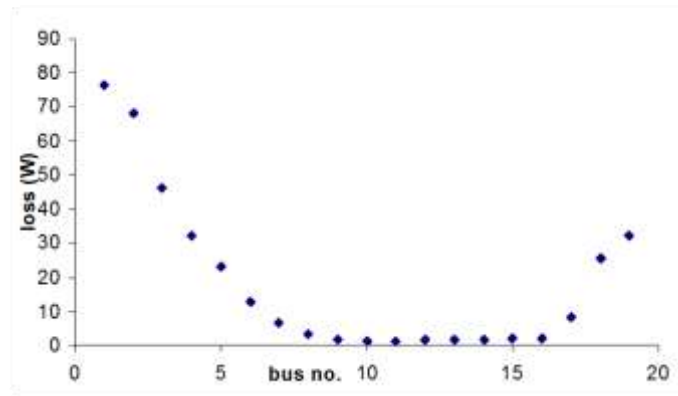


451
 452 **Figure 18.** Spatial distribution load and optimal location of PV source obtained for the Rajmachi system.



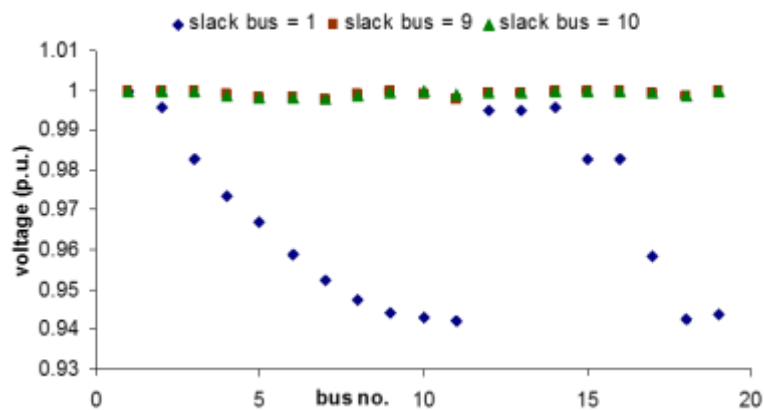
453
 454
 455
 456
 457
 458
 459
 460
 461
 462
 463 **Figure 19.** Network structure obtained for the Rajmachi system using simulated annealing. Also indicated is
 464 the actual location of PV source onsite.

465
 466 Figure 20 shows the variation of losses and Figure 21 gives the variation of voltage profile with
 467 respect to location of the PV system resulting from the parametric analysis. Even for the
 468 comparatively low total connected load, the losses amount to around 5% of the load value. The
 469 improvement in losses is very high (around 98%, from 76 W to 2 W) when the location of the PV
 470 source is changed from bus no. 1 to bus no. 10 (identified as optimal from centre of moments analysis).
 471 The voltage profile also shows considerable improvement on varying the location of the PV source.
 472 With the present location even at a nominal load of 1.5 kW the voltage at the bus furthest from the
 473 source is 0.95 p.u. This indicates that when the system operates at even half the total load rating, the
 474 voltage at the last nodes/buses will be lesser than 0.95 (which is the minimum statutory voltage limit).
 475 This result also matches with the actual voltage at the furthest house point measured experimentally.
 476 For the actual system in Rajmachi, the houses are clustered in the midst of the village which makes it
 477 difficult for the placement of the PV system close to bus no. 10.



478
479

Figure 20: Variation of losses with location of PV system in the Rajmachi system.

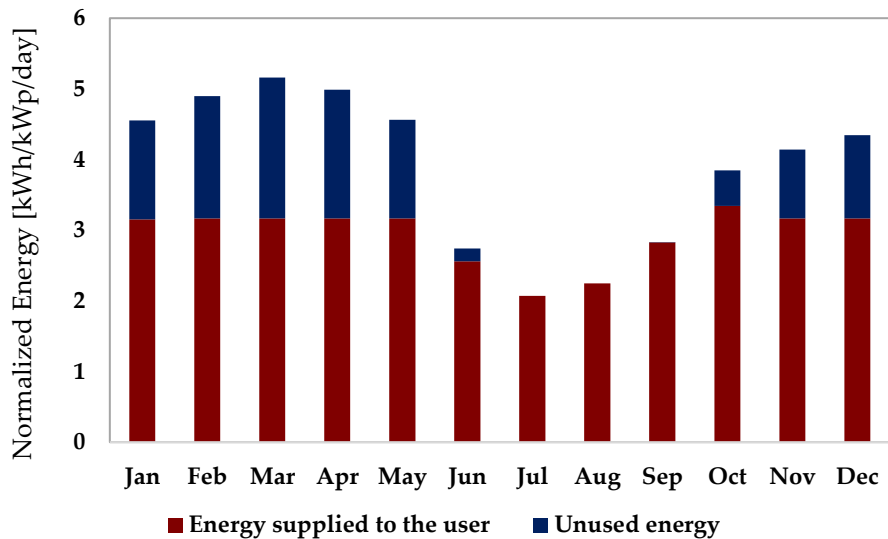


480
481

Figure 21. Voltage profile for different locations of PV system in the Rajmachi system.

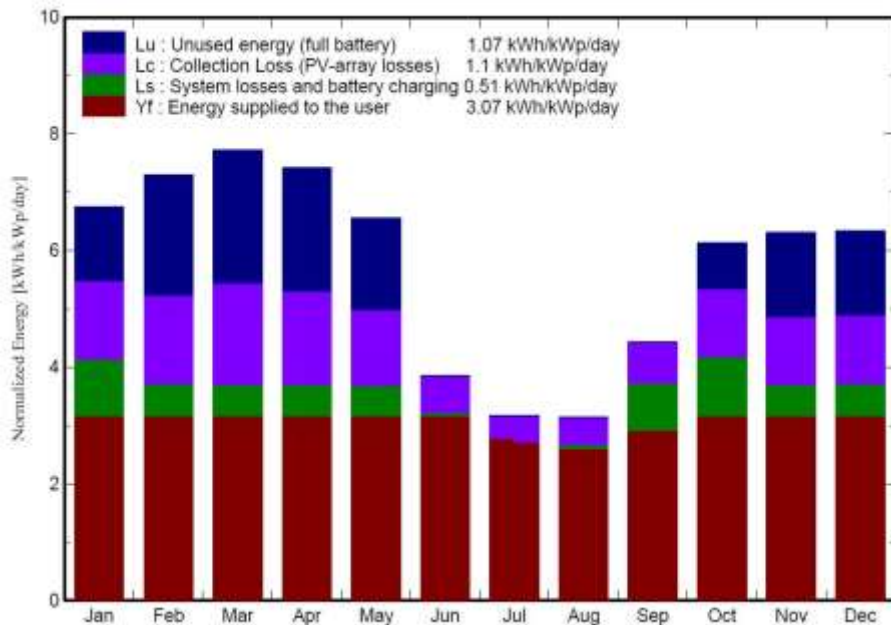
482 5.1.1. Central PV system design

483 The PV system and battery sizes (8.9 kWp and 48V, 5400 Ah respectively) obtained from pre-
 484 sizing were used as inputs to both PVsyst™ and PVGIS5 online software. The meteorological data of
 485 Rajmachi village (Latitude 18.826°N, Longitude 73.396°E) was imported into PVsyst™ from the
 486 PVGIS Climate SAF database. Figure 22 shows the monthly PV energy output simulated by PVGIS5
 487 for a typical meteorological year normalised per kWp. Figure 23 shows the monthly PV energy output
 488 estimates normalised per kWp obtained from the detailed PVsyst™. The PV array size had to be
 489 increased to 9 kWp to match with commercial module specifications from 8.9 kWp. The figure also
 490 shows PV array losses (due its orientation, module temperature and insolation coefficients etc.), the
 491 rest of system losses (due to Maximum Power Point Tracking (MPPT), due to battery charging and
 492 discharging etc.) and PV energy unused (due to battery being fully charged). A detailed description
 493 of the losses and the calculation methodology is available on PVsyst’s user manual and the software
 494 vendor’s website.



495
496

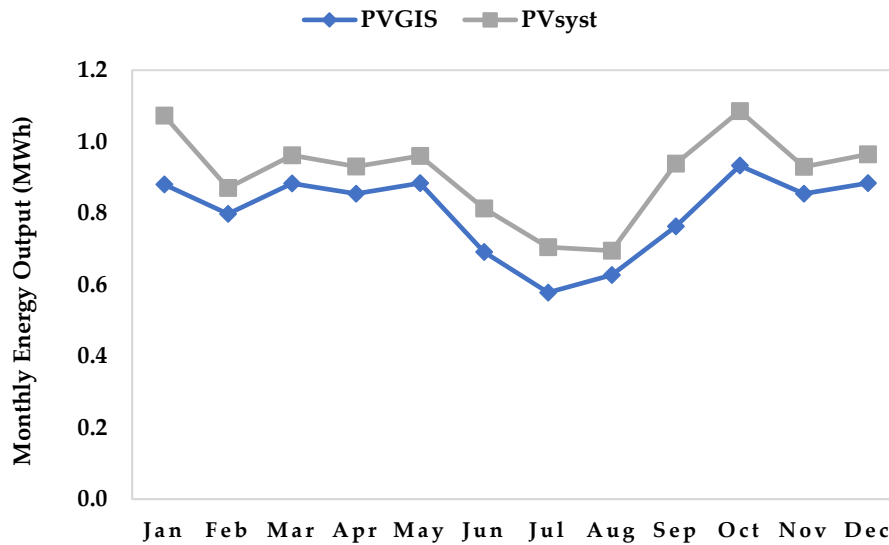
Figure 22. PVGIS5 Monthly PV energy output estimates.



497
498

Figure 23. PVsyst per day monthly PV energy output estimates normalised per kWp.

499 The seasonal variation in PV energy output obtained from both software are very similar. From
 500 a comparison of the monthly energy outputs as shown in Figure 24, it was observed that the output
 501 estimated by PVGIS is marginally lower than that from PVsyst™. Over the year, PVGIS energy
 502 outputs were 12% lower than PVsyst™ on average. This is expected as the PVsyst™ design is detailed
 503 and uses data of commercially available PV modules and batteries whilst PVGIS is based on generic
 504 PV and battery models. As PVGIS online tool does not overestimate PV generation potential, it could
 505 be a viable alternative in the absence of detailed design software like PVsyst™.



506

507

Figure 24. Comparison of PVGIS and PVsyst monthly outputs.

508

509

510

511

512

It was noticed from both PVsyst™ and PVGIS simulations that the ratings of the PV system and battery from pre-sizing were inadequate for supplying the load. As per PVsyst™ calculations the system design would lead to a shortage of 0.32 MWh/year. The design was modified to alleviate energy shortage for the consumers and the final rating of the PV array was found to be 9.9 kWp and the battery bank rating 48V, 7200 Ah. The main parameters of the system are shown in Table 3.

513

Table 3. The main parameters of the central PV system from the final PVsyst design.

| Parameter | Value |
|--|-----------------------------------|
| PV module technology | Monocrystalline Silicon |
| Manufacturer and model | Ecosol PV tech Mono 75Wp 36 cells |
| No. of PV modules in series | 4 |
| No. of parallel strings | 33 |
| Array nominal (STC) power | 9.9 kWp |
| MPPT converter maximum and European efficiencies | 97% / 95% |
| Battery technology | Lead acid |
| Battery bank voltage | 48V |
| Nominal capacity | 7200Ah |
| Number of units | 24 in series x 8 in parallel |

514

515

5. Conclusions

516

517

518

519

520

521

522

523

524

525

Microgrids based on a central PV system could be a potential way forward for the electrification of isolated remote villages in developing countries. This is subject to the country having a good solar resource. PV technology is particularly suited for remote location with difficult terrains due to the modularity of the technology and the lowering technology costs. It was identified that unlike larger isolated power systems, rural microgrids have a low energy demand as the loads are mainly residential and street lighting. Hence these microgrids could be of a single phase configuration. The literature on microgrids and the standard test distribution network are for three phase systems with high power factor, which is not the case for rural microgrids in developing countries. Furthermore, the typical procedure followed currently by planners of rural networks is not comprehensive as it does not consider the importance of PV source siting and optimisation of network structure.

526 The centre of moments approach (section 3.2) can be used for identifying the optimal location of
527 the central PV source in a rural microgrid. The determination of network structure is a complex
528 problem owing to the number of variables to be considered such as location map, terrain information,
529 conductor costs etc. It can be solved as an optimisation problem using simulated annealing. Load
530 flow analysis can determine voltage profiles and power losses. Hence a parametric analysis based on
531 load flow can confirm the PV source location for the network structure developed. Hence an
532 improved PV microgrid design procedure was introduced in this work based on these methods and
533 survey of existing isolated power systems. Two isolated remote villages in India with existing PV
534 microgrids namely Ghotiya village, Chattisgarh and Rajmachi village, Maharashtra are used as case
535 studies. The case study of Ghotiya village was used to formulate the design procedure and that of
536 Rajmachi village to illustrate the design procedure. A comparison of industrial standard PV system
537 design software PVsyst™ and free online tool PVGIS5 from JRC indicated that PVGIS5 could be a
538 viable alternative for designing the central PV system in the microgrid. At present, water-pumping
539 and other irrigation loads in remote villages are fed by independent standalone PV systems. Future
540 work will focus on their integration into the village microgrid.

541 **Author Contributions:** Conceptualization, S.B.; Data collection, S.B.; Network related analysis, S.B.; PV related
542 analysis, G.P.; Methodology, S.B. and G.P.; Project administration and Resources, S.B.; Validation, S.B. and G.P.;
543 Writing-original draft, G.P.; Writing-review & editing, S.B. and G.P.

544 **Funding:** This research received no external funding.

545 **Acknowledgments:** S.B. thanks Prof. Rangan Banerjee, Department of Energy Science and Engineering, IIT
546 Bombay and Prof. S. V. Kulkarni, Department of Electrical Engineering, IIT Bombay for their technical advice.
547 Both authors thank TATA BP Solar, India for the case study data and project site access.

548 **Conflicts of Interest:** The authors declare no conflict of interest.

549

550 References

- 551 1. World Bank, Sustainable Energy for All database. Available online:
552 <https://data.worldbank.org/indicator/EG.ELC.ACCS.ZS> (accessed on 31 July 2018).
- 553 2. Forbes. Available online: [https://www.forbes.com/sites/suparnadutt/2018/05/07/modi-announces-100-](https://www.forbes.com/sites/suparnadutt/2018/05/07/modi-announces-100-village-electrification-but-31-million-homes-are-still-in-the-dark/#2333f11b63ba)
554 [village-electrification-but-31-million-homes-are-still-in-the-dark/#2333f11b63ba](https://www.forbes.com/sites/suparnadutt/2018/05/07/modi-announces-100-village-electrification-but-31-million-homes-are-still-in-the-dark/#2333f11b63ba) (accessed on 31 July 2018).
- 555 3. Sastry, E.V.R. Village electrification programme in India. In proceedings of the 3rd World Conference on
556 Photovoltaic Energy Conversion, 2003; IEEE; Volume 3, pp. 2125-2128.
- 557 4. Hubble, A.H.; Ustun, T.S. Composition, placement, and economics of rural microgrids for ensuring
558 sustainable development. *Sustainable Energy, Grids and Networks* **2018** Volume 13, pp. 1-18,
559 <https://doi.org/10.1016/j.segan.2017.10.001>.
- 560 5. Theo, W.L.; Lim, J.S.; Ho, W.S.; Hashim, H.; Lee, C.T. Review of distributed generation (DG) system
561 planning and optimisation techniques: Comparison of numerical and mathematical modelling methods.
562 *Renewable and Sustainable Energy Reviews* **2017**, Volume 67, pp. 531-573,
563 <https://doi.org/10.1016/j.rser.2016.09.063>.
- 564 6. Diesendorf, M.; Elliston, B. The feasibility of 100% renewable electricity systems: A response to critics.
565 *Renewable and Sustainable Energy Reviews* **2018**, Volume 93, pp. 318-330,
566 <https://doi.org/10.1016/j.rser.2018.05.042>.
- 567 7. Jiang, T.; Costa, L.; Tordjman, P.; Venkata, S.S.; Siebert, N.; Kumar, J.; Puttgen, H.B.; Venkataraman, A.;
568 Dutta, S.; Li, Y.; Tang, T. A Microgrid Test bed in Singapore: An electrification project for affordable access
569 to electricity with optimal asset management. *IEEE Electrification Magazine* **2017**, Volume 5(2), pp.74-82,
570 <https://doi.org/10.1109/MELE.2017.2685978>.
- 571 8. Planas, E.; Andreu, J.; Gárate, J.I.; de Alegría, I.M.; Ibarra, E. AC and DC technology in microgrids: A
572 review. *Renewable and Sustainable Energy Reviews* **2015**, Volume 43, pp.726-749,
573 <https://doi.org/10.1016/j.rser.2014.11.067>.
- 574 9. Jordehi, A.R. Allocation of distributed generation units in electric power systems: A review. *Renewable and*
575 *Sustainable Energy Reviews* **2016**, Volume 56, pp.893-905., <https://doi.org/10.1016/j.rser.2015.11.086>.

- 576 10. Abdmouleh, Z.; Gastli, A.; Ben-Brahim, L.; Haouari, M.; Al-Emadi, N.A. Review of optimization techniques
577 applied for the integration of distributed generation from renewable energy sources. *Renewable Energy* **2017**,
578 *Volume 113*, pp.266-280, <https://doi.org/10.1016/j.renene.2017.05.087>.
- 579 11. Hilton, G.; Cruden, A.; Kent, J., Comparative analysis of domestic and feeder connected batteries for low
580 voltage networks with high photovoltaic penetration. *Journal of Energy Storage* **2017**, *Volume 13*, pp.334-343.,
581 <https://doi.org/10.1016/j.est.2017.07.019>.
- 582 12. Aman, M.M.; Jasmon, G.B.; Bakar, A.H.A.; Mokhlis, H. A new approach for optimum simultaneous multi-
583 DG distributed generation Units placement and sizing based on maximization of system loadability using
584 HPSO (hybrid particle swarm optimization) algorithm. *Energy* **2014**, *Volume 66*, pp.202-215,
585 <https://doi.org/10.1016/j.energy.2013.12.037>.
- 586 13. Kefayat, M.; Ara, A.L.; Niaki, S.N. A hybrid of ant colony optimization and artificial bee colony algorithm
587 for probabilistic optimal placement and sizing of distributed energy resources. *Energy Conversion and*
588 *Management* **2015**, *Volume 99*, pp.149-161., <https://doi.org/10.1016/j.enconman.2014.12.037>.
- 589 14. Adefarati, T.; Bansal, R.C. Integration of renewable distributed generators into the distribution system: a
590 review. *IET Renewable Power Generation* **2016**, *Volume 10*(7), pp.873-884, [http://dx.doi.org/10.1049/iet-](http://dx.doi.org/10.1049/iet-rpg.2015.0378)
591 [rpg.2015.0378](http://dx.doi.org/10.1049/iet-rpg.2015.0378).
- 592 15. Prakash, P.; Khatod, D.K. Optimal sizing and siting techniques for distributed generation in distribution
593 systems: A review. *Renewable and Sustainable Energy Reviews* **2016**, *Volume 57*, pp.111-130,
594 <https://doi.org/10.1016/j.rser.2015.12.099>.
- 595 16. Asmuth, P.; Verstege, J.F. Optimal network structure for distribution systems with microgrids. In
596 Proceedings of International Conference on Future Power Systems; IEEE: 2005.
- 597 17. Willis, H.L. *Power Distribution Planning Reference Book*, 2nd ed.; Marcel Dikker, USA, 2004.
- 598 18. Pabla, A.S. *Electric power distribution*, 6th ed.; Tata McGraw-Hill, India, 2012.
- 599 19. Gouin, V.; Alvarez-Hérault, M.C.; Raison, B. Optimal planning of urban distribution network considering
600 its topology. In CIRED 2015-The 23rd International Conference on Electricity Distribution; CIRED: 2015.
- 601 20. Wolfram Mathworld. Available online: <http://mathworld.wolfram.com/SimulatedAnnealing.html>
602 (accessed on 31 July 2018).
- 603 21. Das, J.C. *Power system analysis: short-circuit load flow and harmonics*, 2nd ed.; CRC Press, USA, 2016.
- 604 22. MATPOWER. Available online: <http://www.pserc.cornell.edu/matpower/> (accessed on 31 July 2018).
- 605 23. Islam, M.; Mekhilef, S. Hasan, M. Single phase transformerless inverter topologies for grid-tied
606 photovoltaic system: A review. *Renewable and Sustainable Energy Reviews* **2015**, *Volume 45*, pp.69-86.,
607 <https://doi.org/10.1016/j.rser.2015.01.009>.
- 608 24. The Satellite Application Facility on Climate Monitoring. Available online:
609 http://www.cmsaf.eu/EN/Home/home_node.html (accessed on 31 July 2018).
- 610 25. PVGIS version 5 release candidate. Available online: <http://re.jrc.ec.europa.eu/PVGIS5-beta.html> (accessed
611 on 31 July 2018).
- 612 26. Pillai, G.; Naser, H.A.Y. Techno-economic potential of largescale photovoltaics in Bahrain. *Sustainable*
613 *Energy Technologies and Assessments* **2018**, *Volume 27*, pp.40-45., <https://doi.org/10.1016/j.seta.2018.03.003>.
- 614 27. Georgitsioti, T. Photovoltaic potential and performance evaluation studies in India and the UK. Doctoral
615 thesis, Northumbria University, UK, 2015.



© 2018 by the authors. Submitted for possible open access publication under the terms and conditions of the Creative Commons Attribution (CC BY) license

618 (<http://creativecommons.org/licenses/by/4.0/>).